JOURNAL OF GEOPHYSICAL RESEARCH, VOL. 99, NO. D1, PAGES 1263–1271, JANUARY 20, 1994

Ozone within the El Chichón aerosol cloud inferred from solar backscatter ultraviolet continuous-scan measurements

Guoyong Wen
Environmental Research Division, Argonne National Laboratory, Argonne, Illinois

John E. Frederick
Department of the Geophysical Sciences, University of Chicago, Chicago, Illinois

Abstract. Large amounts of SO_2 injected into the stratosphere by the El Chichón volcanic eruption greatly enhanced the sulfuric acid aerosol loading. According to laboratory studies, the increase in aerosol surface area would lead to a loss of ozone. Radiation measurements from the solar backscatter ultraviolet spectroradiometer are used to probe the absorbing and scattering properties of the stratosphere after the eruption. The backscattered radiation is enhanced for wavelengths greater than 290 nm, with a peak at about 302 nm. The enhancements associated with aerosol backscattering and ozone change can be separated. A decrease in column ozone of 8 to 30 Dobson units was deduced within the aerosol layer at an altitude between 20 and 30 km following the month of the eruption.

Introduction

The El Chichón (17.3°N, 93.2°W) eruption in late March and early April 1982 injected about 3.3×10^6 tons of SO_2 into the stratosphere [*Krueger*, 1983]. As volcanic SO_2 is the principal precursor of stratospheric aerosol, a major volcanic eruption will consequently enhance the stratospheric aerosol loading. A great deal of attention has focused within recent years on the effects of a volcanic eruption on stratospheric ozone. Laboratory studies have found that heterogeneous chemical reactions could take place on the surfaces of sulfuric aerosol particles, releasing chlorine, denitrifying the atmosphere, and destroying ozone as a consequence. Low ozone amounts have been reported from several stations after the eruption [*Bais et al.*, 1985; *DeLuisi et al.*, 1985; *Deutsch*, 1985; *Komhyr et al.*, 1985]. Theoretical studies of the impact of a volcanic eruption on stratospheric ozone were presented by *Hofmann and Solomon* [1989], *Brasseur and Granier* [1992], and *Brasseur et al.* [1990]. Nonetheless, the problem of how volcanic aerosol might affect stratospheric ozone remains poorly understood.

This work uses solar backscatter ultraviolet (SBUV) continuous-scan measurements together with a radiative transfer model based on the discrete-ordinate method [*Stamnes et al.*, 1988] to investigate backscattered UV radiation after the El Chichón eruption and the associated changes in atmospheric composition. Since the El Chichón aerosol cloud was confined to the latitude band between the equator and 30°N in the first couple of months after the eruption [*Thomas et al.*, 1983; *Barth et al.*, 1983], the investigation will be focused on using the backscattered UV radiation to infer changes in the lower stratosphere at low latitudes during the early stage of the El Chichón aerosol cloud.

Paper number 93JD02661.
0148-0227/94/93JD-02661$05.00

Data Description

The SBUV instrument was launched on the Nimbus 7 satellite on October 24, 1978. The satellite was at an altitude of about 955 km in a Sun-sychronous polar orbit, having local noon (ascending) and midnight (descending) equator crossings and 26.1° of longitudinal separation between orbits. The orbital period is about 104.16 min. The SBUV experiment consists of a double Ebert-Fastie spectrometer and a filter photometer to measure the ultraviolet Earth radiance and solar irradiance. The continuous mode of the spectrometer scans the spectrum from 160 to 400 nm sampling data at 80-ms intervals in 0.2-nm increments with a 1.1-nm half-width triangular bandpass, while the photometer measures solar irradiance and Earth radiance with a 3-nm-wide wavelength band centered at 343.3 nm. Both spectrometer and photometer simultaneously view identical fields of solar radiation scattered by the terrestrial atmosphere in the nadir direction. The instantaneous field of view is 11.33° × 11.33° for both the spectrometer and the photometer. The SBUV instruments operated in the continuous-scan mode on 1 day during each 24-day period [*Heath et al.*, 1978]. The uncertainties in the continuous-scan data, including the error due to instrument calibration and the wavelength-dependent drifts with time due to changes in instrument properties, are less than 2.6% for wavelengths greater than 290 nm [*Schlesinger et al.*, 1988].

Since the instrument measures radiance in the nadir direction only, we define a directional albedo as the ratio of backscattered radiance and the incident solar radiation normalized by the cosine of solar zenith angle to eliminate geometrical effects. This is

$$\alpha_\lambda = \frac{\pi I_\lambda(\theta_0,\ \theta = 0)}{F_{0\lambda} \cos\theta_0}, \tag{1}$$

where I_λ and $F_{0\lambda}$ are the backscattered UV radiance in the vertical direction (polar angle $\theta = 0$) and the incident solar irradiance with a solar zenith angle θ_0 at wavelength λ,

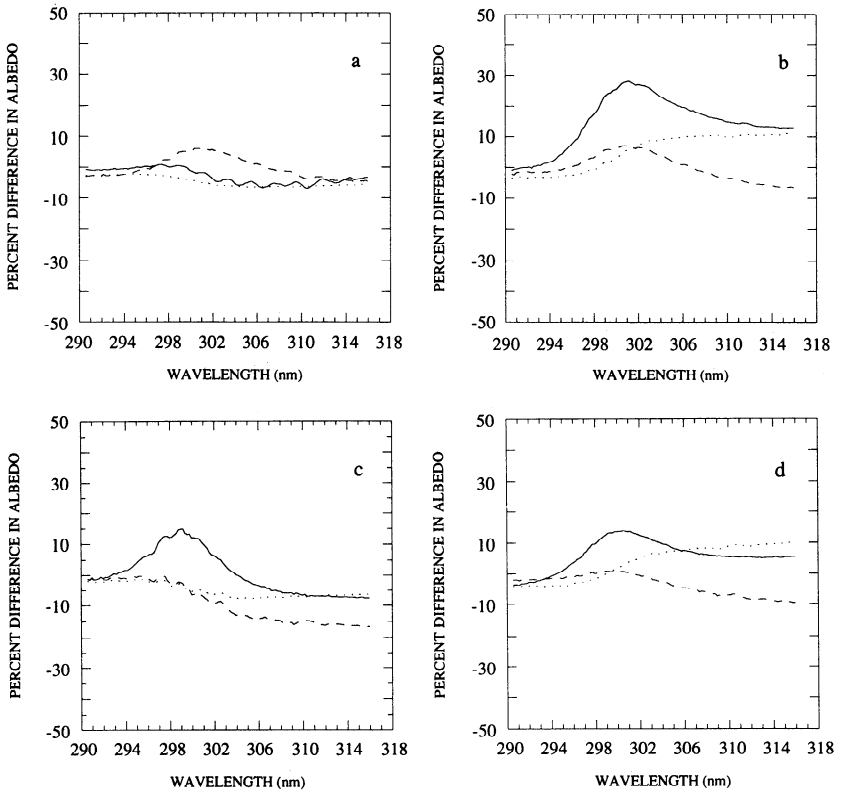

Figure 1. The percent change in averaged spectral albedos in the latitude band 10°–20°N after the El Chichón eruption for 1982 (solid curve), 1983 (dashed curve), and 1984 (dotted curve) compared to those measured during the same months in 1981. (a) April 15; (b) May 9; (c) June 3; (d) June 27.

respectively. The normalizing factor π is used such that for a hemispherically isotropic radiance, the directional albedo is the real albedo. The directional albedo will be used throughout this paper.

Observational Results

It is well known that the volcanic eruption injected a large amount of SO_2 into the stratosphere [*Krueger*, 1983; *McPeters and Heath*, 1984]. Eventually, the gaseous SO_2 will be converted to sulfate aerosol particles, providing sites for heterogeneous chemical reactions. Both scattering by the aerosol and the possible ozone reduction due to heterogeneous chemical reactions act to increase the backscattered UV radiation. In turn, measured changes in backscattered UV radiation carry information on the abundances of scatterers and absorbers.

First, we examined changes in backscattered UV radiation after the eruption. Figure 1 compares the spectral albedos after the eruption, in 1982, 1983, and 1984, to the averaged albedos from 1981. All albedos measured in the latitude band 10°–20°N on a single day have been averaged together, and percent changes after the eruption have been computed. Since the local time beneath the satellite is always local noon in daylight, the different scans in the averages have nearly the same solar zenith angle. The absorption structure from SO_2 shows clearly on April 15, 1982, while no clear SO_2 absorption structure exists in the averaged spectral albedos on May 9, 1982, and after. However, a large enhancement of backscattered spectral albedos appears for wavelengths greater than 294 nm on May 9, 1982, and 1 month later, with a peak at about 301 nm within the latitude band from the equator to 30°N (only measurements within 10° to 20°N are plotted in Figure 1). The dissipation of SO_2 absorption structure and the consequent enhancement of the backscattered UV radiation are consistent with gas to particle conversion taking place in a period of 1 to 2 months and a possible ozone reduction during that period. It is evident in Figure 1 that the albedos measured between April and June of 1982 are anomalous in comparison to the corresponding months in 1983 and 1984. Some structure also appears on the curve for June 3, 1983. However, the wavelength dependence of this structure is not consistent with SO_2 absorption. The cause of this structure is not clear.

A quantitative understanding of the mechanisms responsible for the enhancement in albedo requires a detailed analysis, because UV radiation at wavelengths greater than 290 nm can penetrate down to the troposphere. The observed backscattered UV radiation emerging at the top of the atmosphere would be affected by ozone amount, aerosol scattering, tropospheric cloud, and even surface reflection. It is not possible to model the daily averaged backscattered UV spectral albedos, because the backscattered UV radiation depends not only on the optical depth of the cloud but also on the cloud height. The averaged albedos and the averaged optical depth are nonlinearly related.

In order to simplify the problem, one spectral scan obtained for a clear atmosphere 1 year before the eruption is chosen as the reference. Since the photometer on the satellite senses radiation at the wavelength 343.3 nm, where ozone absorption is very small, the photometer measure-

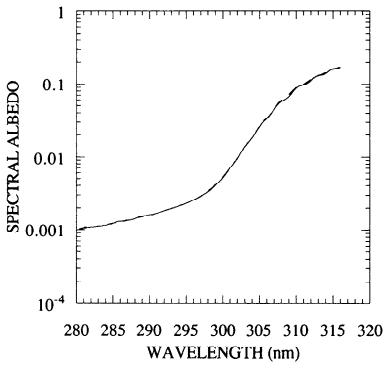

Figure 2. SBUV spectral albedos (solid curve, 20.3°N, 82.8°E, on May 14, 1981) compared with model results (dashed curve) having total column ozone of 288 DU, cosine of solar zenith angle $\mu_0 = 0.994$, and surface albedo of 0.05.

ments can be used to identify tropospheric clouds in the SBUV field of view. The criterion for a clear scene is that both the photometer measurements and their fluctuations be small as the satellite moves over the geographic region of interest. In this case, the radiative transfer model is able to reproduce the measured spectral albedo with a maximum difference at each wavelength of less than 1%. The spectral albedos in Figure 2 are the clear atmosphere reference and the model simulation for a total ozone of 288 Dobson units (DU) and a surface albedo of 0.05. The discrete-ordinate radiative transfer model used in this calculation included 16 streams. Since the measured clear-atmosphere spectral albedos are the references for comparisons with other data, the corresponding computed spectral albedos are used as references in the model study.

The percent difference between individual measured spectral albedos and the reference are presented in Figures 3, 4, and 5 for about 10 days before, 10 days after, and 1 month after the El Chichón eruption, respectively. Before the eruption (Figure 3), the spectral albedos at wavelengths shorter than 296 nm have little variability, and the large variation of spectral albedos at wavelengths greater than 296 nm is due to tropospheric clouds, as one would expect. The SO_2 absorption structures appear on April 15, 1982 (Figure 4), the first day after the eruption during which the SBUV continuous mode was in operation. Similar to the scans before the eruption, the spectral albedos at wavelengths shorter than 296 nm were not affected. Only a small enhancement appeared in a couple of scans at wavelengths near 296 nm. However, the spectral albedos at wavelengths shorter than 296 nm were enhanced tremendously for some but not all scans on May 9, 1982 (Figure 5), about 1 month after the eruption. The enhancement in spectral albedos starts at wavelength 290 nm and has a peak 30 to 80% above the reference scan at about 302 nm.

The increase of backscattered UV radiation can arise from an increase in scatterers such as the El Chichón aerosol particles, from decreases in absorbers, or from both. Scattering by tropospheric clouds is also a factor which affects the emergent UV radiation at the top of the atmosphere. The following sections analyze mechanisms that could enhance the backscattered UV radiation and propose an objective

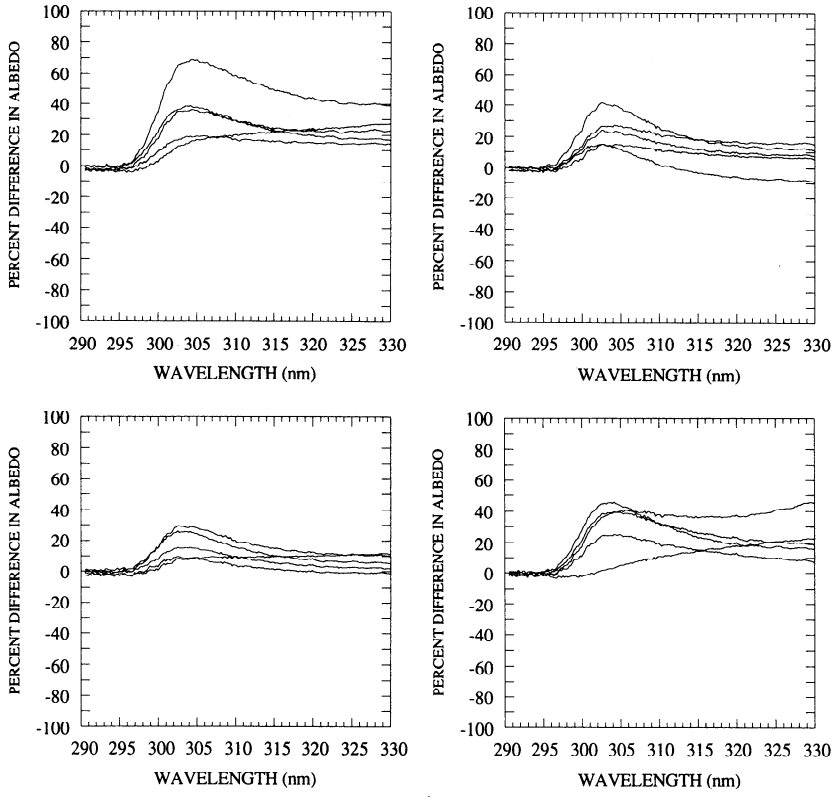

Figure 3. The percent difference for individual-scan spectral albedos on March 22, 1982, in the latitude band 10° to 20°N compared to the reference scan (20.3°N, 82.8°E, on May 14, 1981).

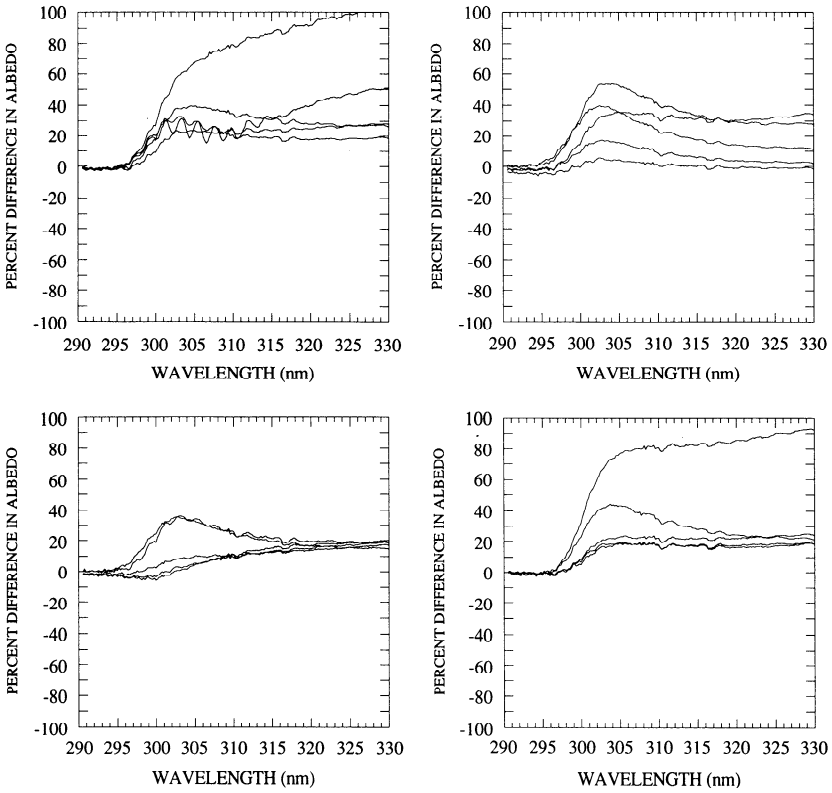

Figure 4. The percent difference for individual-scan spectral albedos on April 15, 1982, in the latitude band 10° to 20°N compared to the same reference scan as in Figure 3.

technique for estimating the aerosol optical depth and the ozone change.

Theoretical Interpretation of Backscattered Radiation

The azimuthally averaged upward intensity I at the top of the atmosphere may be expressed as

$$I(\tau = 0;\ \mu) = I(\tau^*;\ \mu)e^{-\tau^*/\mu} + \int_0^{\tau^*} S(\tau;\ \mu)e^{-\tau/\mu}\,\frac{d\tau}{\mu}, \tag{2}$$

where τ is the optical depth and μ is the cosine of the polar angle, τ^* is the total optical depth of the atmosphere, and S is the source function for scattering [*Chandrasekhar*, 1960]. The quantities I, τ, and S depend on wavelength. The first and the second terms in (2) represent the lower boundary contribution and the internal atmospheric contribution, respectively. Since the optical depth is a function of altitude, the intensity in the vertical direction at the top of the atmosphere can be written as

$$I(\tau = 0;\mu = 1) = \int_0^{\infty} C(z)\ dz, \tag{3}$$

where $C(z)$ is called the contribution function. Usually, the contribution function is normalized such that the maximum value is unity. The contribution functions for a typical low-latitude atmosphere are presented in Figure 6. The spectral dependence of changes in backscattered UV radiation from a perturbed layer between z_1 and z_2 may be characterized through the fraction of the total contribution attributed to scattering from that layer, that is,

$$Q(z_1,\ z_2) = \frac{\displaystyle\int_{z_1}^{z_2} C(z)\ dz}{\displaystyle\int_0^{\infty} C(z)\ dz.} \tag{4}$$

For a layer of fixed thickness located at a high altitude, Q monotonically decreases with wavelength because most radiation at longer wavelengths passes through the layer with little absorption and scattering, while at low altitude, Q monotonically increases with wavelength because most radiation at shorter wavelengths is absorbed at higher altitudes. It is also expected that at some intermediate altitude, the contribution from a layer increases with wavelength, reaches a maximum, and then decreases. The contribution function from a layer is helpful in understanding the relationship between a disturbance, for example, a decline in ozone in the layer and the changes in radiance measured by SBUV. The larger the contribution function from a layer at a given wavelength, the larger the change in the backscattered radiance that would occur for any disturbance. Figure 7 shows the contribution function for a layer between 20 and 30 km. With the peak at about 301 nm, the shape of the fractional contribution is similar to the observed enhancement of spectral albedos after the El Chichón eruption.

The contribution function from a layer qualitatively explains the enhancement in the backscattered UV radiation.

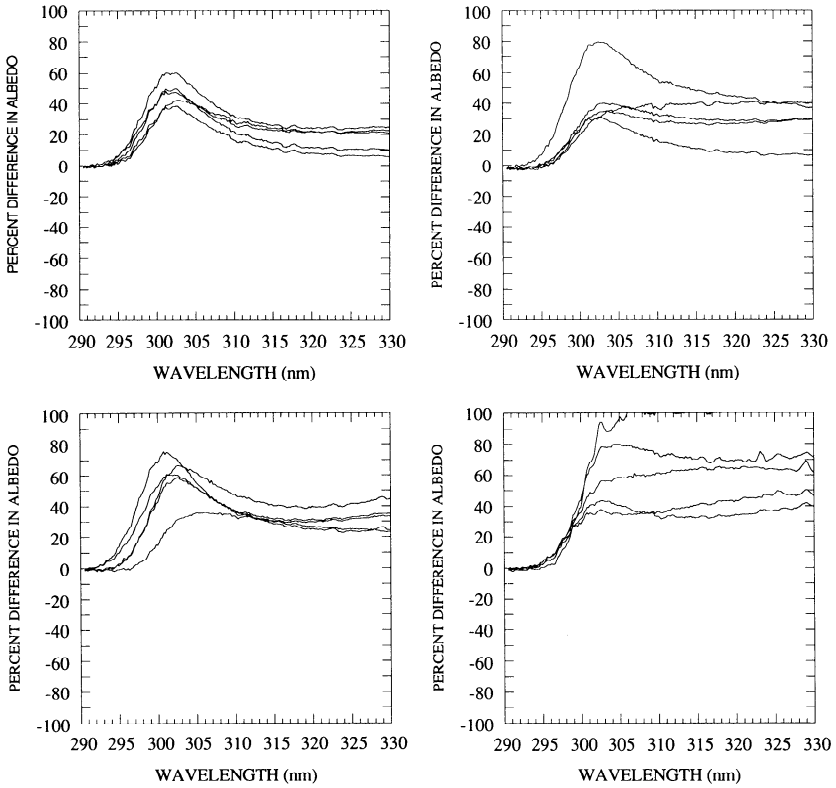

Figure 5. The percent difference for individual-scan spectral albedos on May 9, 1982, in the latitude band 10° to 20°N compared to the same reference scan as in Figure 3.

The quantitative description of the enhancement must include the optical properties of the disturbed layer. The following sections analyze the mechanisms that cause the enhancement.

Enhancement of Spectral Albedo Due to Aerosol Backscattering

The El Chichón aerosol size distribution is a function of altitude and varies with time. The likely spatial and temporal inhomogeneities in the aerosol size distribution make it impossible to model the El Chichón aerosol phase function precisely. The phase function generated using the observed size distribution at about 25 km in altitude [*Hofmann and Rosen*, 1984] and Mie theory [*Bohren and Huffman*, 1983] is taken to represent the scattering properties of the El Chichón aerosol.

Like most polydispersion Mie scatterers, the El Chichón aerosols have a unique phase function with a strong peak within about 11° of the forward direction and a sharp increase in the backward direction. Figure 8 illustrates the adopted phase function. The El Chichón aerosol phase function differs dramatically, especially in a backward direction, from the analytic Henyey-Greenstein phase function [*Henyey and Greenstein*, 1941], which is often used for

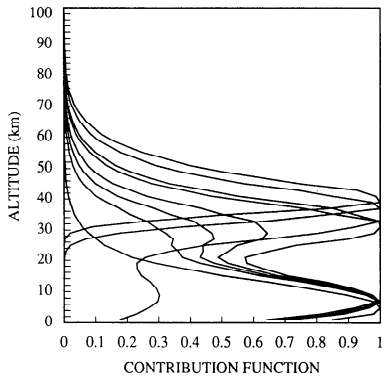

Figure 6. Contribution function for an atmosphere with total ozone of 300 DU and a cosine of solar zenith angle of 0.9. The curves from top to bottom are for wavelengths 290.5, 294.5, 300.5, 302.5, 303.5, 304.5, 305.5, and 314.5 nm.

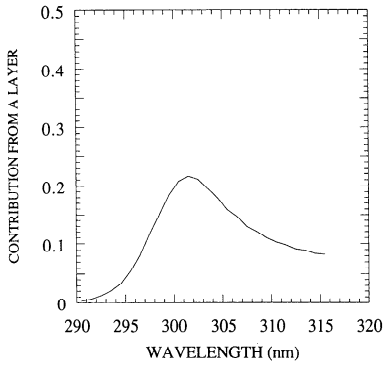

Figure 7. The fractional contribution from a layer at an altitude between 20 and 30 km for the same atmosphere as in Figure 6.

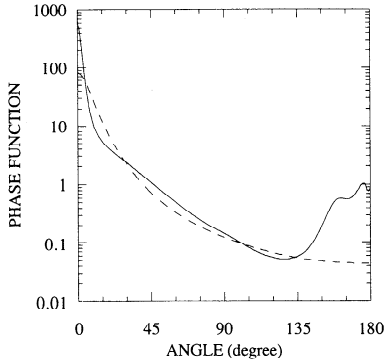

Figure 8. The phase function of El Chichón aerosol (solid curve) and Henyey-Greenstein phase function with an asymmetry factor of 0.85 (dashed curve).

computing hemispheric fluxes. Since the SBUV spectrometer looks straight down, observing radiances and taking measurements in the nadir direction, and the El Chichón aerosol clouds are restricted in latitude from 0° to 30°N, where the sun is nearly overhead for the Nimbus 7 satellite, the instrument measures almost straight backscattered radiation. The realistic aerosol phase function is necessary for describing the backscattered UV radiation.

For the radiative transfer calculation, the aerosol layer is assumed to reside between 20 and 30 km in altitude and to have plane parallel stratification. For a given column ozone amount, the statistical relationship derived by *Bojkov* [1969] is used to estimate the vertical profile. The lower surface is assumed to be a Lambertian reflector. For a given ozone distribution, the vertical profile of aerosol optical thickness is adjusted such that the modeled enhancement in backscattered UV radiation matches the observation near the peak. The discrete-ordinate radiative transfer model uses 32 streams for this calculation.

Two scans of spectral albedo are selected to represent a cloud-free atmosphere based on the degree of homogeneity in photometer measurements. By choosing different aerosol optical depths, the model produces a maximum enhancement of backscattered UV radiation similar to the measurements. However, Figure 9 shows that the modeled enhancements based on aerosol scattering alone have a very different spectral dependence from the observations. Although the bigger aerosol optical depth may simulate the observation near the peak of the enhancement at about 302 nm, it overestimates the measured enhancements in the longer-wavelength tail. The smaller aerosol optical depth in the model, however, generates the observed enhancement in the tail near 325–330 nm but underestimates the enhancements at shorter wavelengths.

The radiative transfer model shows that the wavelength and magnitude of the peak enhancement are determined by the vertical distribution of aerosol optical depth. However, the computed enhancements of spectral albedo for wavelengths greater than 310 nm are much less dependent on the vertical profile of aerosol optical depth. For wavelengths greater than 310 nm, the spectral variation of the simulated enhancement is small, while the measured enhancement shows a considerable decrease with wavelength.

A potential explanation for the discrepancy in Figure 9 could be a wavelength dependence in aerosol scattering. However, we reject this possibility on the following basis. Ground-based measurements of El Chichón aerosol optical depth at Mauna Loa [*DeLuisi et al.*, 1983] show an increase with wavelength for wavelengths shorter than 550 nm. With the aerosol particle concentration used earlier, the extinction based on Mie theory shows that the optical depth of the aerosol layer increases by less than 1% from 310 to 330 nm.

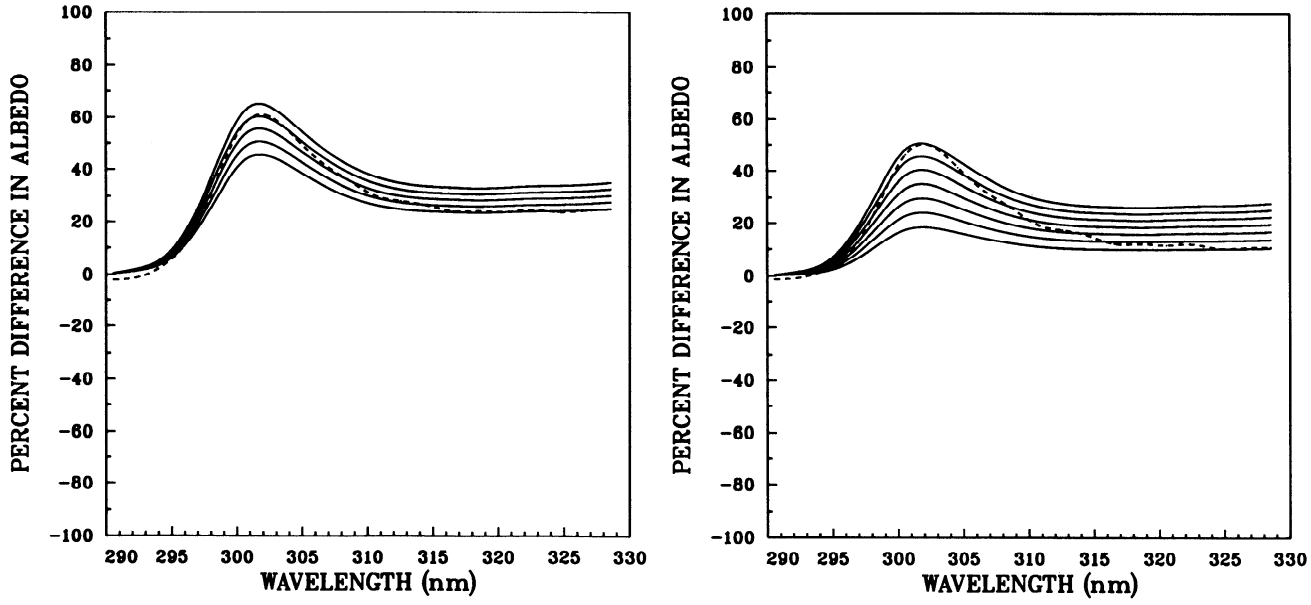

Figure 9. Comparison of observation (dashed curve) and model (solid curves) results for an aerosol layer at an altitude between 20 and 30 km with different optical depths. (Left) 16°N, 49°E; May 9, 1982; optical depths of 0.4, 0.45, 0.5, 0.55, and 0.6 from lower to upper curves; (right) 17°N, 23°E; May 9, 1982; optical depths of 0.15, 0.2, 0.25, 0.3, 0.35, 0.4, and 0.45 from lower to upper curves.

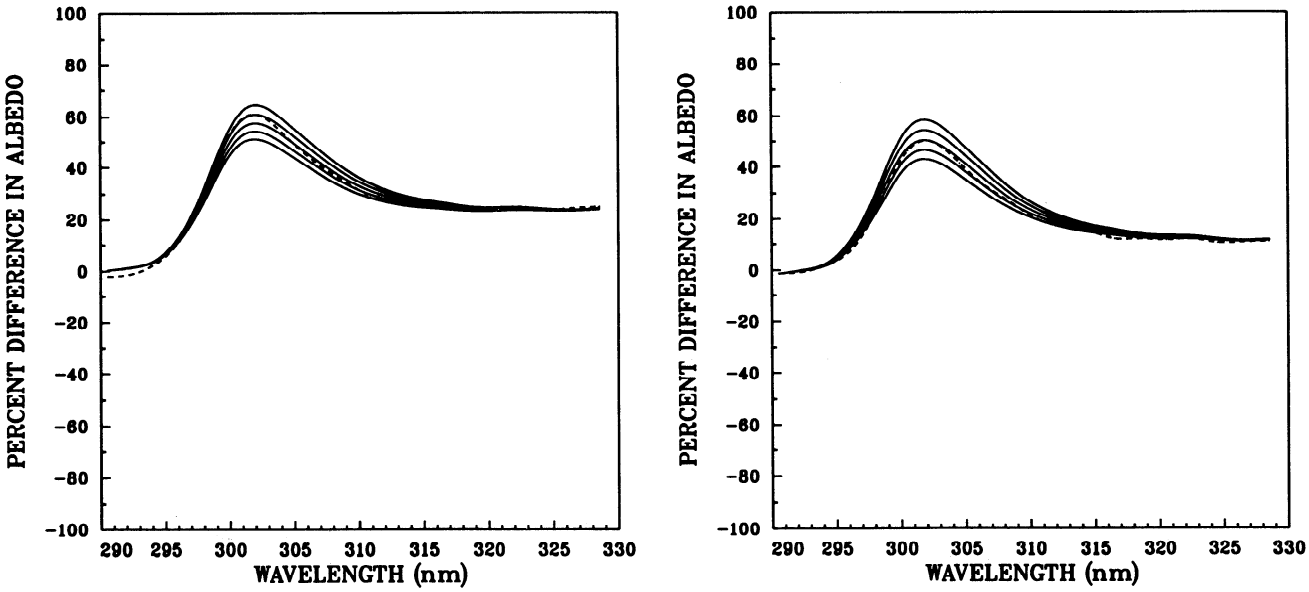

Figure 10. The observed (dashed curve) and modeled (solid curves) enhancements in spectral albedos, including both aerosol scattering and an ozone decrease ΔO_3 in percentage of unperturbed amount of 288 DU. (left) May 9, 1982; 16°N, 49°E; aerosol optical depth = 0.37 and ΔO_3 = 3, 4, 5, 6, and 7% from the lower to the upper solid curve; (right) May 9, 1982; 17°N, 23°E; aerosol optical depth = 0.15 and ΔO_3 = 7, 8, 9, 10, and 11% from the lower to the upper solid curve.

Because the enhancement of spectral albedo for wavelengths from 310 to 330 nm depends only weakly on the vertical distribution of aerosol optical depth and the aerosol optical depth varies very little over the wavelength region concerned, the enhancement due to the aerosol backscattering will have little spectral dependence. The inconsistency between the modeled results and the observations indicates that a mechanism in addition to aerosol backscattering is required to account for the enhanced spectral albedos. A decrease in the ozone abundance appears to be a likely explanation.

Evidence for Ozone Decrease After the El Chichón Eruption

As shown previously, the aerosol layer alone is able to produce the observed enhancement either at the peak or at the tail of the spectrum but fails to simulate the observations over the whole wavelength region. Another candidate for explaining the enhancement in the backscattered UV radiation could be ozone decline. The effect of an ozone decrease on the atmosphere's spectral properties differs from that of the aerosol layer even though both act to enhance the backscattered UV radiation. The absorption cross section of ozone decreases rapidly with wavelength. From 310 to 330 nm, the ozone absorption cross section decreases by more than 1 order of magnitude [*Molina and Molina*, 1986]. On the other hand, the Rayleigh scattering cross section is proportional inversely to the fourth power of the wavelength. Any ozone decrease would lead to a greater increase in the single scattering albedo at shorter wavelengths than at longer wavelengths. Hence an ozone decrease would enhance the backscattered UV radiation more efficiently at shorter wavelengths than at longer wavelengths.

In addition to the assumptions used above in the study for an aerosol layer, a region with depleted ozone is assumed to coincide with this aerosol. Since more ozone decrease is expected with more sulfuric acid aerosol, the vertical profile of ozone destruction is taken to be proportional to the local aerosol abundance. As wavelength increases, the ozone absorption cross section decreases quickly; hence the enhancement will asymptotically approach the enhancement due to the aerosol layer alone at longer wavelength. The enhancement at longer wavelength may be used to estimate the aerosol optical depth, and the ozone decline will contribute additional enhancement for shorter wavelengths.

For clear skies, the surface albedo and aerosol optical depth may be obtained by comparing the observed radiance at 330 nm and simultaneous photometer measurements with modeled results. Then the amount of ozone decrease and its vertical profile are adjusted such that the modeled enhancements fit the observed backscattered radiance at shorter wavelengths.

The modeled enhancement due to the combined aerosol backscattering and ozone decrease closely simulates the observations over the whole wavelength region from 290 to 330 nm. Figure 10 shows that with aerosol optical depths in the range 0.15 to 0.4, which are consistent with observations at Mauna Loa [*DeLuisi et al.*, 1983], an ozone decrease of 8 to 30 DU at an altitude between 20 and 30 km is needed to reproduce the observed enhancements in albedo.

The derived ozone decrease in the aerosol layer is free from error related to the form of the aerosol phase function because the aerosol optical depths are small and single scattering is the primary contribution to the radiation fields. The error in the phase function from the unknown vertical profile of aerosol concentration may affect the retrieval of aerosol optical depth to some extent, but the inferred ozone deficit is not expected to be sensitive to this.

Discussion

The different spectral signatures of aerosol scattering and ozone decrease in the measured SBUV albedo are consistent with a decline in ozone levels during the month after the El Chichón eruption. The aerosol optical depth was estimated by using spectral albedo near 330 nm and simultaneous photometer measurements at 343 nm. The ozone decrease within the aerosol layer is estimated from the spectral enhancement of backscattered radiation observed by the SBUV instrument.

Although the SBUV measurements show a clear sign of ozone decrease when interpreted using the radiative transfer model, the mechanisms causing the decrease remain undefined. The change in ozone could be due to heterogeneous chemical reactions on aerosol surfaces, the radiatively driven circulation and associated transport, or both. Since the gaseous volcanic emissions are composed largely of water vapor and carbon dioxide, low levels of ozone in the volcanic air plume are expected immediately upon injection of the plume into the stratosphere. However, no clear ozone deficit appeared in the early stage of the plume at higher altitudes, as is evidenced by the lack of enhanced albedo at wavelengths less than 296 nm in Figure 4. The SBUV measurements also indicate that most of the SO_2 was concentrated in the lower stratosphere (about 20 km); that is, very little absorption by SO_2 appeared at wavelengths less than 296 nm.

The El Chichón aerosol layer plays a role in climate perturbation by cooling the Earth's surface, reflecting sunlight, and heating the stratosphere by the trapping of thermal radiation [*Hofmann*, 1987; *McCracken and Luther*, 1984; *Robock*, 1984; *Vupputuri and Blanchet*, 1984). Radiosonde data in the tropics have shown a warming of the stratosphere after the El Chichón eruption [*Labitzke and Naujokat*, 1984]. By trapping upwelling thermal radiation, the El Chichón aerosol layer itself would be warmed and lifted. Hence the ozone-poor air mass in the volcanic plume would be carried to a higher altitude.

In addition, mixing could take place as a result of wind shear acting on the vertically inhomogeneous aerosol distribution. The mixing process could play an important role in redistributing ozone and the aerosols vertically. The evolution of the El Chichón aerosol cloud observed by the Solar Mesosphere Explorer satellite [*Thomas et al.*, 1983] provides additional evidence for the action of mixing. Since there was no clear sign of an enhancement in spectral albedo on April 15, 1982, due to either aerosols or ozone changes, the ozone decrease within the aerosol layer observed on May 9, 1982, may arise from a combination of heterogeneous chemistry, convective motions, and mixing, as mentioned earlier.

Conclusion

The SBUV continuous scan measurements are useful in studying the impact of the El Chichón volcanic eruption on the lower stratosphere. The backscattered UV radiation was enhanced at short wavelengths 1 month after the eruption, indicating changes in the optical properties of the stratosphere. The enhancements also show a clear wavelength dependence. Based on interpretation by the radiative transfer model, the satellite measurements imply ozone decreases of 8 to 30 DU at altitudes between 20 and 30 km 1 month after the eruption. The technique developed here can also be used to investigate backscattered UV radiation after the Pinatubo eruption.

Acknowledgments. Implementation of the radiative transfer model was supported in part by NASA grant NAG5-873. The authors thank K. Stamnes for providing a copy of the discrete-ordinate code.

References

Bais, A. F., C. S. Zerefos, I. C. Zioma, N. Zoumakis, H. T. Mantis, D. J. Hofmann, and G. Fiocco, Decreases in the ozone and the SO_2 columns following the appearance of the El Chichón aerosol cloud at mid-latitude, in *Atmospheric Ozone, Proceedings of the Quatrennial Ozone Symposium*, pp. 353–356, D. Reidel, Norwell, Mass., 1985.

Barth, C. A., R. W. Sanders, R. J. Thomas, G. E. Thomas, B. M. Jakosky, and R. A. West, Formation of the El Chichón aerosol cloud, *Geophys. Res. Lett.*, *10*, 993–996, 1983.

Bohren, C. F., and D. R. Huffman, *Absorption and Scattering of Light by Small Particles*, John Wiley, New York, 1983.

Bojkov, R. D., Computing the vertical ozone distribution from its relationship with total ozone amount, *J. Appl. Meteorol.*, *8*, 284–292, 1969.

Brasseur, G. P., and C. Granier, Mount Pinatubo aerosols, chlorofluorocarbons and ozone depletion, *Science*, *257*, 1239–1242, 1992.

Brasseur, G. P., C. Granier, and S. Walters, Future changes in stratospheric ozone and the role of heterogeneous chemistry, *Nature*, *348*, 626–628, 1990.

Chandrasekhar, S., *Radiative Transfer*, Dover, Mineola, N. Y., 1960.

DeLuisi, J. J., E. G. Dutton, K. L. Coulson, T. E. DeFoor, and B. G. Mendonca, On some radiative features of the El Chichón volcanic stratospheric dust cloud and a cloud of unknown origin observed at Mauna Loa, *J. Geophys. Res.*, *88*, 6769–6772, 1983.

DeLuisi, J. J., C. L. Mateer, and W. D. Komhyr, Effects of the El Chichón stratospheric aerosol cloud on Umkehr measurements at Mauna Loa, Hawaii, in *Atmospheric Ozone, Proceedings of the Quatrennial Ozone Symposium*, pp. 316–320, D. Reidel, Norwell, Mass., 1985.

Deutsch, H. U., Total ozone trend in the light of ozone sounding, the impact of El Chichón, in *Atmospheric Ozone, Proceedings of the Quatrennial Ozone Symposium*, pp. 263–268, D. Reidel, Norwell, Mass., 1985.

Heath, D., A. J. Krueger, and H. Park, in *The Nimbus 7 User's Guide*, pp. 175–211, NASA, Goddard Space Flight Center, Greenbelt, Md., 1978.

Henyey, L. G., and J. L. Greenstein, Diffuse radiation in the galaxy, *Astrophys. J.*, *93*, 70–83, 1941.

Hofmann, D. J., Perturbation of the global atmosphere associated with the El Chichón volcanic eruption of 1982, *Rev. Geophys.*, *25*, 743–759, 1987.

Hofmann, D. J., and J. M. Rosen, Balloonborne particle counter observation of the El Chichón aerosol layers in the 0.01–1.8 μm radius range, *Geofis. Int.*, *23-2*, 155–185, 1984.

Hofmann, D. J., and S. Solomon, Ozone destruction through heterogeneous chemistry following the eruption of El Chichón, *J. Geophys. Res.*, *94*, 5029–5041, 1989.

Komhyr, W. D., S. J. Oltmans, A. N. Chopra, R. K. Leonard, T. E. Garcia, and C. McFee, Results of Umkehr, total ozone, and sulfur dioxide observations in Hawaii following the eruption of El Chichón volcano in 1982, in *Atmospheric Ozone, Proceedings of the Quatrennial Ozone Symposium*, pp. 305–310, D. Reidel, Norwell, Mass., 1985.

Krueger, A. J., Sighting of El Chichón sulfur dioxide clouds with the Nimbus 7 total ozone mapping spectrometer, *Science*, *220*, 1377–1379, 1983.

Labitzke, K., and B. Naujokat, On the effects of the volcanic eruptions of Mount Agung and El Chichón on the temperature of the stratosphere, *Geofis. Int.*, *23-2*, 223–232, 1984.

McCracken, M. C., and F. M. Luther, Preliminary estimate of the radiative and climate effects of the El Chichón eruption, *Geofis. Int.*, *23-3*, 385–401, 1984.

McPeters, R. D., and D. F. Heath, Satellite observation of SO_2 from El Chichón: Identification and measurement, *Geophys. Res. Lett.*, *11*, 1203–1206, 1984.

Molina, L. T., and M. J. Molina, Absolute absorption cross section of ozone in the 185- to 350-nm wavelength range, *J. Geophys. Res.*, *91*, 14,501–14,508, 1986.

Robock, A., Climate model simulation of the effects of the El Chichón eruption, *Geofis. Int.*, *23-3*, 403–414, 1984.

Schlesinger, B. M., R. P. Cebula, D. F. Heath, and A. J. Fleig, Nimbus 7 solar backscatter ultraviolet (SBUV) spectral scan solar irradiance and Earth radiance product user's guide, *NASA Ref. Publ. 1199*, pp. 5–24, 1988.

Stamnes, K., S. Tsay, W. Wiscombe, and K. Jayaweera, Numerically stable algorithm for discrete-ordinate-method radiative transfer in multiple scattering and emitting layered media, *Appl. Opt.*, *27*, 2502–2509, 1988.

Thomas, G. E., B. M. Jakosky, R. A. West, and R. W. Sanders, Satellite limb-scanning thermal infrared observations of the El Chichón stratospheric aerosol: First results, *Geophys. Res. Lett.*, *10*, 997–1000, 1983.

Vupputuri, R. K. R., and J. P. Blanchet, The possible effects of El Chichón eruption on atmospheric thermal and chemical-structure and surface climate, *Geofis. Int.*, *23-3*, 433–447, 1984.

J. E. Frederick, Department of the Geophysical Sciences, University of Chicago, 5734 South Ellis Avenue, Chicago, IL 60637.

G. Wen, Environmental Research Division, Argonne National Laboratory, 9700 South Cass Avenue, Argonne, IL 60439.

(Received April 28, 1993; revised September 7, 1993; accepted September 16, 1993.)